Time evolution of Gaussian-type initial conditions associated with the Davey - Stewartson equations

1996 J. Phys. A: Math. Gen. 29 4237

(http://iopscience.iop.org/0305-4470/29/14/040)

J. Phys. A: Math. Gen. **29** (1996) 4237–4245. Printed in the UK

Time evolution of Gaussian-type initial conditions associated with the Davey–Stewartson equations

Katsuhiro Nishinari†‖, Tetsu Yajima‡¶ and Takenobu Nakao§

† Department of Mechanical Engineering, Faculty of Engineering, Yamagata University, Jyonan 4-3-16, Yonezawa-shi, Yamagata 992, Japan

‡ Department of Applied Physics, Faculty of Engineering, University of Tokyo, Hongo 7-3-1, Bunkyo-ku, Tokyo 113, Japan

§ IBM Japan Ltd, 1623-14, Shimotsuruma, Yamato-shi, Kanagawa 242, Japan

Received 2 January 1996

Abstract. The Cauchy problem of the Davey–Stewartson equations with non-trivial boundaries is studied. Initial conditions for the equations are chosen to have Gaussian-type envelope shapes, and the time evolution is investigated both theoretically and numerically. It is found that an initial packet grows and oscillates radiating ripples, then a localized structure called a dromion appears asymptotically. It is also observed that the ripples run away mainly along the mean flows. The results of numerical simulations and the analysis by the inverse scattering transform show good agreement with each other.

1. Introduction

In recent years the Davey–Stewartson (DS) 1 equations [1]

$$\mathrm{i}q_t + q_{xx} + q_{yy} + (U+V)q = 0 \tag{1.1a}$$

$$U = \int_{-\infty}^{y} \mathrm{d}y' \, (|q|^2)_x + u(x,t) \qquad V = \int_{-\infty}^{x} \mathrm{d}x' \, (|q|^2)_y + v(y,t) \tag{1.1b}$$

have attracted a good deal of interest in various physical problems. The subscripts in (1.1) denote the partial derivatives with respect to the indicated variables. The functions $u(x,t)$ and $v(x,t)$ in (1.1*b*) are determined by the boundary conditions of the system. If u and v are not identically zero, these equations have a solution called a dromion which localizes in two spatial dimensions [2]. The variable q, hereafter called the main flow, localizes while U and V, hereafter called the mean flows, are driven at the boundaries like one-dimensional solitons [3]. The dromion solution comes from the interaction between the main flow and the mean flows. Since the DS1 equations can be derived in many branches of physics, such as fluid dynamics [4] or plasma physics [5], these localized structures are useful for many practical cases.

Although studies of mathematical properties of the dromion solution have been done intensively until the present [6], detailed research on the emergence of dromions from an initial arbitrary wavepacket has not yet been performed. As for soliton equations in one dimension, such as the Korteweg–de Vries (KdV) equation and the nonlinear Schrödinger

‖ E-mail address: knishi@dips.yz.yamagata-u.ac.jp

¶ E-mail address: yajimat@mmm.t.u-tokyo.ac.jp

0305-4470/96/144237+09$19.50

(NLS) equation, the initial-value problem is well studied by the inverse scattering transform (IST) [1] or numerical analyses [7]. These analyses show that solitons emerge from an initial wavepacket emitting radiations. In these one-dimensional equations, solitons have their origins from the zeros of scattering data, while dromions do not. Since dromions come from the focusing effect of boundaries, the effect of boundary conditions can be considered to play an important role in their formation.

In our previous papers [8–10] we have made detailed studies on the collision of two single dromions and on the stability of dromions against perturbations to find that the mean flows play an important role in controlling localized structures of the main flow. The purpose of this paper is to investigate the initial-value problem of the DS1 equations under non-trivial boundary conditions which are the same as those of the one-dromion solution. We are going to study the emergence of dromions from Gaussian-type initial conditions by using both the IST and numerical simulations.

This paper is organized as follows. In section 2, we summarize the IST of the DS1 equations and present some theoretical results concerning our problem. The numerical results of the initial-boundary value problem are given in section 3. Comparison of the numerical results with the result given in section 2 is considered in section 4. Concluding discussions are given in section 5.

2. The IST associated with the DS1 equations

Let us summarize the IST of the DS1 equations [6] related to the problem considered in this paper. Equations (1.1) are associated with the Lax equation

$$[L_1, L_2] \equiv L_1 L_2 - L_2 L_1 = 0. \tag{2.1}$$

The quantities L_1 and L_2 are 2×2 matrices. If we write the complex conjugate of q to be q^*, they are defined as

$$L_1 = \begin{pmatrix} \partial_x & \dfrac{1}{\sqrt{2}} q \\ -\dfrac{1}{\sqrt{2}} q^* & \partial_y \end{pmatrix} \tag{2.2a}$$

$$L_2 = \mathrm{i}\partial_t + \begin{pmatrix} 1 & 0 \\ 0 & -1 \end{pmatrix} (\partial_y - \partial_x)^2 - \begin{pmatrix} 0 & \sqrt{2} q_y \\ -\sqrt{2} q_x^* & 0 \end{pmatrix} (\partial_y - \partial_x) + \begin{pmatrix} V - \sqrt{2} q_y \\ -\sqrt{2} q_x^* - U \end{pmatrix}. \tag{2.2b}$$

First we fix the variable t and consider the spectral problem

$$L_1 \Psi = 0 \tag{2.3}$$

where Ψ is a 2×2 matrix function. By using another matrix M, we express Ψ as

$$\Psi \equiv M(x, y, k) \exp\left[\mathrm{i}k \begin{pmatrix} -y & 0 \\ 0 & x \end{pmatrix} \right] = M(x, y, k) \begin{pmatrix} \mathrm{e}^{-\mathrm{i}ky} & 0 \\ 0 & \mathrm{e}^{\mathrm{i}kx} \end{pmatrix}. \tag{2.4}$$

We can see from (2.2*a*), (2.3) and (2.4) that each element of M satisfies

$$(M_{11}^{\pm})_x = -\frac{1}{\sqrt{2}} q M_{21}^{\pm} \tag{2.5a}$$

$$(M_{12}^{\pm} \mathrm{e}^{-\mathrm{i}kx})_x = -\frac{1}{\sqrt{2}} q M_{22}^{\pm} \mathrm{e}^{-\mathrm{i}kx} \tag{2.5b}$$

$$(M_{21}^{\pm} \mathrm{e}^{\mathrm{i}ky})_y = \frac{1}{\sqrt{2}} q^* M_{11}^{\pm} \mathrm{e}^{\mathrm{i}ky} \tag{2.5c}$$

$$(M_{22}^{\pm})_y = \frac{1}{\sqrt{2}} q^* M_{12}^{\pm} \tag{2.5d}$$

where M^+ and M^- are analytic in the upper and lower half complex k plane, respectively. The eigenfunctions $M^{\pm}$ are related via the scattering equations,

$$\begin{pmatrix} M_{11}^+(k) \\ M_{21}^+(k) \end{pmatrix} - \begin{pmatrix} M_{11}^-(k) \\ M_{21}^-(k) \end{pmatrix} = \int_{-\infty}^{\infty} \mathrm{d}l\, T(k,l) \exp[-\mathrm{i}(lx+ky)] \begin{pmatrix} M_{12}^+(l) \\ M_{22}^+(l) \end{pmatrix} \tag{2.6a}$$

$$\begin{pmatrix} M_{12}^+(k) \\ M_{22}^+(k) \end{pmatrix} - \begin{pmatrix} M_{12}^-(k) \\ M_{22}^-(k) \end{pmatrix} = -\int_{-\infty}^{\infty} \mathrm{d}l\, S(k,l) \exp[\mathrm{i}(kx+ly)] \begin{pmatrix} M_{11}^-(l) \\ M_{21}^-(l) \end{pmatrix}. \tag{2.6b}$$

The scattering data $S(k,l)$ and $T(k,l)$ are given by

$$S(k,l) = \frac{1}{2\sqrt{2}\pi} \int_{-\infty}^{\infty} \mathrm{d}x \int_{-\infty}^{\infty} \mathrm{d}y\, q M_{22}^-(k) \exp[-\mathrm{i}(kx+ly)] \tag{2.7a}$$

and

$$T(k,l) = -S^*(l,k). \tag{2.7b}$$

Equations (2.6) define a non-local Riemann–Hilbert problem whose solution yields $M^{\pm}$ in terms of S. Substituting the solution of this problem into (2.5) and taking the limit $k \to \infty$, we can reconstruct the potential q as

$$q(x,y) = \frac{1}{\sqrt{2}\pi} \int_{-\infty}^{\infty} \mathrm{d}k \int_{-\infty}^{\infty} \mathrm{d}l\, S(k,l) \exp[\mathrm{i}(kx+ly)] M_{11}^-(l). \tag{2.8}$$

Now we consider the time development of the system. The associated t part of the Lax pair is given by (2.2*b*). We can see from (2.7*a*) that $q(x,y)$ is proportional to the Fourier transform of $S(k,l)$, hereafter written as $\hat{S}(x,y)$, in the linear limit. Then from (1.1*a*) we find that it evolves according to

$$\mathrm{i}\hat{S}_t + \hat{S}_{xx} + \hat{S}_{yy} + (u+v)\hat{S} = 0 \tag{2.9a}$$

where

$$\hat{S}(x,y,t) \equiv \frac{1}{2\pi} \int_{-\infty}^{\infty} \mathrm{d}k \int_{-\infty}^{\infty} \mathrm{d}l\, S(k,l) \exp[\mathrm{i}(kx+ly)]. \tag{2.9b}$$

Equations (2.5)–(2.9) provide the IST for the DS1 equations. Given $q(t=0)$, u and v, then (2.5) and (2.7*a*) yield $S(t=0)$ and (2.9*a*) yields $S(t=t)$. The solution of the Riemann–Hilbert problem gives $M^{\pm}$ and finally (2.8) gives $q(t)$.

Assuming u and v do not depend on t, i.e. $u(x,t) = u(x)$ and $v(y,t) = v(y)$, and setting $\hat{S}(x,y,t) = T(t)X(x)Y(y)$, we have a set of equations from (2.9*a*):

$$T' + \mathrm{i}(m^2+n^2)T = 0 \tag{2.10a}$$

$$X'' + u(x)X = -m^2 X \qquad Y'' + v(y)Y = -n^2 Y \tag{2.10b}$$

where m and n are constants which give eigenvalues. The analysis of (2.10*b*) is closely related to the well known spectral theory of the stationary Schrödinger equation. We use $X(x;m)$ and $X_j(x)$ to express the normalized eigenfunctions of the derivative operator in the left-hand side of the first equation of (2.10*b*); the function $X(x;m)$ is the eigenfunction which belongs to a continuous eigenvalue spectrum m and $X_j(x)$ is the one belonging to discrete eigenvalues $m = \mathrm{i}m_j$, $j = 1, \ldots, M$. The eigenfunctions $Y(y;n)$, $Y_j(y)$ and the

eigenvalues $n = \mathrm{i}n_h$, $h = 1, \ldots, N$ are defined similarly. The general theory of the Sturm–Liouville eigenvalue problem assures that these eigenfunctions form an orthonormal system. Then the solution of (2.9*a*) is given by

$$\begin{aligned}\hat{S}(x, y, t) = &\sum_{j=1}^{M}\sum_{h=1}^{N} \rho_{jh} X_j(x) Y_h(y) \exp[\mathrm{i}(m_j^2 + n_h^2)t] \\ &+ \int_{-\infty}^{\infty} \mathrm{d}m \int_{-\infty}^{\infty} \mathrm{d}n\, \rho X(x; m) Y(y; n) \exp[-\mathrm{i}(m^2 + n^2)t] \\ &+ \int_{-\infty}^{\infty} \mathrm{d}m \left\{ \sum_{j=1}^{M} \rho_j X_j(x) Y(y; m) \exp[\mathrm{i}(m_j^2 - m^2)t] \right. \\ &\left. + \sum_{h=1}^{N} \bar{\rho}_h X(x; m) Y_h(y) \exp[\mathrm{i}(n_h^2 - m^2)t] \right\}. \end{aligned} \tag{2.11}$$

Considering the orthogonality of the eigenfunctions, we can get the coefficients ρ_{jh} from the initial data:

$$\rho_{jh} = \int_{-\infty}^{\infty} \mathrm{d}x \int_{-\infty}^{\infty} \mathrm{d}y\, \hat{S}(x, y, 0) X_j^*(x) Y_h^*(y) \tag{2.12}$$

and ρ, ρ_j and $\bar{\rho}_j$ are given similarly [6].

The method of steepest descent implies the following asymptotic behaviour of $\hat{S}$ in time:

$$\hat{S}(x, y, t) \sim \sum_{j=1}^{M}\sum_{h=1}^{N} \rho_{jh} X_j(x) Y_h(y) \exp[\mathrm{i}(m_j^2 + n_h^2)t] \qquad \text{as } t \to \infty. \tag{2.13}$$

This result plays an important role in the discussions in the following sections. If $\hat{S}$ is expressed as (2.13), we can calculate q in a closed form. The solution corresponds to the so-called (M, N) 'breather dromion' [6]. This fact implies that *any* initial conditions generate solutions that will be breather dromions asymptotically, if $u(x)$ and $v(y)$ provide discrete eigenvalues. The initial condition only fixes the constant ρ_{jh} through (2.12).

3. Numerical analyses of the initial-boundary-value problem

So far we have considered the initial-boundary-value problem theoretically by using the IST. In order to make detailed analyses on the time evolution of the initial wavepacket, we must investigate the initial-boundary-value problem by using numerical simulations.

First, we present the initial and the boundary conditions adopted for simulations. We have chosen a Gaussian-type function as an initial condition for q:

$$q(x, y, 0) = a \exp[-\mu(x^2 + y^2) + \mathrm{i}\theta_0]. \tag{3.1}$$

The parameters a, μ and θ_0 are real constants. We have also defined the functions u and v given at the boundaries as

$$u(x) = \frac{2\lambda^2}{\cosh^2(\lambda x)} \qquad v(y) = \frac{2\lambda^2}{\cosh^2(\lambda y)} \tag{3.2}$$

where λ is a real parameter. These boundary conditions correspond to those of the one dromion solution [11], i.e. the functions u and v are 'reflectionless potentials' of (2.10*b*) under $M = N = 1$. Then the result of section 2 implies that the initial condition (3.1) becomes one-dromion in the limit of $t \to \infty$.

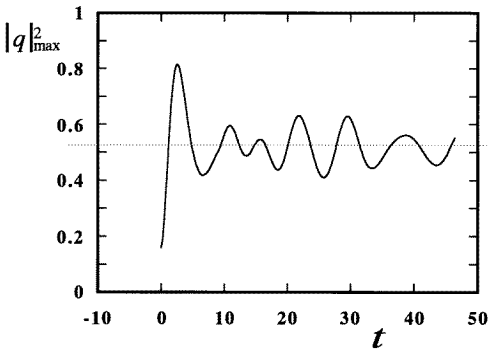

Figure 1. The maximum amplitude of $|q|^2$ when the initial condition is given as $q = 0.4e^{-0.05(x^2+y^2)+0.1i}$.

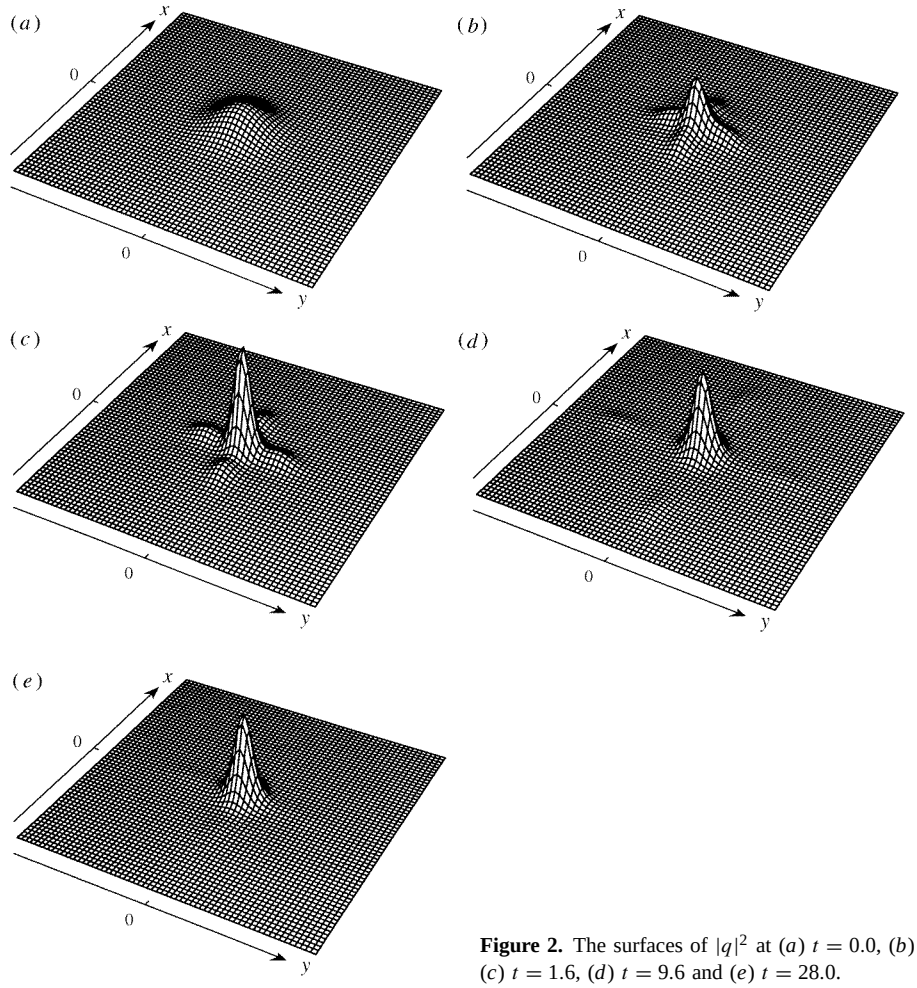

Figure 2. The surfaces of $|q|^2$ at (*a*) $t = 0.0$, (*b*) $t = 0.8$, (*c*) $t = 1.6$, (*d*) $t = 9.6$ and (*e*) $t = 28.0$.

Next, we describe the numerical method briefly [9]. The computation region $[-p, p] \times [-p, p]$ is transformed into $[0, 2\pi] \times [0, 2\pi]$ by transformations $x \to \pi(x+p)/p$ and $y \to \pi(y+p)/p$, and a grid has been taken 64×64. We take p as 15 throughout simulations. The numerical integration of (1.1) has been performed by using the pseudospectral method with periodic boundary condition. Time integration is performed by both the Burilsh and Store

method and the fourth-order Runge–Kutta method with appropriate accuracy of adaptive step size control. To prevent the reflection of the ripples due to the periodic boundaries, we have set an absorbing area and diminish the time derivatives of the main flow. The width of the area is a 10-point wide mesh from the boundaries of the grid, and the damping factor increases linearly from the inner sides of the absorbing area to its boundaries [12].

We fixed the values of the parameters in (3.1) and (3.2) as $\lambda = 0.8$, $a = 0.4$, $\mu = 0.05$ and $\theta_0 = 0.1$. Figure 1 shows a typical aspect of time evolution of the maximum amplitude of $|q|^2$, hereafter denoted by $|q|^2_{\max}$. We can observe that it increases in the initial stage, and oscillates irregularly around a certain value in the course of time. We performed numerical calculation until the average of $|q|^2_{\max}$ becomes clear and the shape of the surface of $|q|^2$ looks like that of one dromion. We can observe from figure 1 that the average is $0.52 \sim 0.54$. Some pictures of the surface of $|q|^2$ are given in figure 2. We can see that the shape of $|q|^2$ becomes almost the same as that of one dromion after $t \sim 28$. Ripples are extracted from the initial wavepacket and they run away to infinity mainly along the mean flows.

4. Comparison of the numerical results with the IST

It is difficult to get the explicit form of $q(x, y, t)$ analytically when the initial condition is given by (3.1) and the boundary conditions $u(x)$ and $v(y)$ by (3.2). However, we can get it in a closed form in the limit of $t \to \infty$. According to the discussion in section 2, $\hat{S}(x, y)$ is given by (2.13) when t goes to infinity, and then we can show that q is given by the sum of the ripples and q_∞ [6], where

$$q_\infty = \frac{2\sqrt{2}\rho\lambda \exp[-\lambda(x+y) + 2\mathrm{i}\lambda^2 t]}{|\rho|^2 + [1+\exp(-2\lambda x)][1+\exp(-2\lambda y)]}. \tag{4.1}$$

We have expressed ρ_{11} as ρ. This means that we have one dromion q_∞ asymptotically.

In order to compare the results of numerical analyses with those of the IST, we must calculate ρ in (4.1) from the initial condition. It is, however, difficult to get the value of ρ analytically. Thus we present the efficient way of calculating the value of ρ numerically in the following.

Substituting (2.7*a*) into (2.9*b*) and integrating with respect to y' and l, we have

$$\hat{S}(x, y) = \frac{1}{2\sqrt{2}\pi} \int_{-\infty}^{\infty} \mathrm{d}k \int_{-\infty}^{\infty} \mathrm{d}x'\, q(x', y) M_{22}^{-} \exp(-\mathrm{i}kx') \exp(\mathrm{i}kx). \tag{4.2}$$

The integral with respect to x' in (4.2) can be performed by using (2.5*b*) and gives

$$\hat{S}(x, y) = \frac{1}{2\pi} \int_{-\infty}^{\infty} \mathrm{d}k\, A(x, y, k)|_{x\to-\infty} \exp(\mathrm{i}kx) \tag{4.3}$$

where we have set $A(x, y, k) = M_{12}^{-} \exp(-\mathrm{i}kx)$. We need $X_j(x)$ and $Y_j(y)$ to get ρ, which are eigenfunctions of (2.10*b*) under the boundary condition (3.2). Writing $\mathrm{e}^{\lambda x} \equiv s$, we can find that X satisfies a equation

$$s^2 X_{ss} + s X_s + \left[\frac{8s^2}{(1+s^2)^2} + \tilde{m}^2\right] X = 0$$

where $\tilde{m} \equiv m/\lambda$. This equation has a solution $X = s/(1+s^2)$, the only one which goes to zero under $s \to 0, \infty$ ($x \to \pm\infty$), when $\tilde{m} = \mathrm{i}$. The function Y can be derived

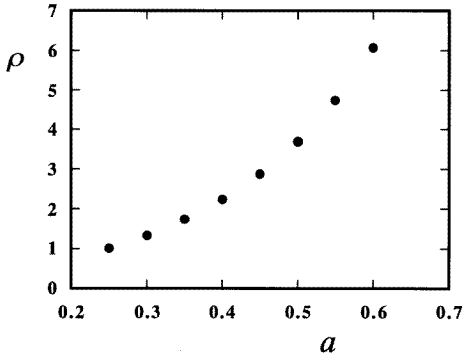

Figure 3. The value of ρ versus the amplitude of the Gaussian-type initial condition when the width of the initial condition is $\mu = 0.05$.

similarly. By suitable normalization of X and Y, we can get discrete eigenvalues and the eigenfunctions which belong to them:

$$X = \frac{\sqrt{\lambda/2}}{\cosh(\lambda x)} \qquad Y = \frac{\sqrt{\lambda/2}}{\cosh(\lambda y)} \tag{4.4}$$
$$m = n = \mathrm{i}\lambda.$$

Substituting (4.3) and (4.4) into (2.12) and integrating with respect to x, we obtain

$$\rho = \frac{1}{4}\int_{-\infty}^{\infty} \mathrm{d}k \int_{-\infty}^{\infty} \mathrm{d}y \ \mathrm{sech}\left(\frac{\pi k}{2\lambda}\right) \mathrm{sech}(\lambda y) A(x, y, k)|_{x\to-\infty}. \tag{4.5}$$

We also express $M_{22}^{-}\exp(-\mathrm{i}kx)$ as $B(x, y, k)$ and get a coupled system from (2.5*b*) and (2.5*d*):

$$A_x = -\frac{1}{\sqrt{2}} q(x, y, 0) B \qquad B_y = \frac{1}{\sqrt{2}} q(x, y, 0)^* A. \tag{4.6}$$

The boundary conditions of A and B are given by

$$A|_{x\to\infty} = 0 \qquad B|_{y\to-\infty} = \exp(-\mathrm{i}kx). \tag{4.7}$$

We can calculate ρ by using (3.1), (4.5), (4.6) and (4.7). We solve (4.6) and get the value $A(x, y, k)|_{x=-\infty}$ numerically, because we cannot solve them analytically under the initial condition (3.1). The value of ρ obtained by the direct simulation is given in figure 3. We have also presented the results in table 1. Considering the asymptotic pulse given by (4.1), we can get the maximum value $|q_\infty|^2_{\max}$ and its integral in the whole space, which is considered to be the volume of the localized structure:

$$|q|^2_{\max} = \frac{2|\rho|^2\lambda^2}{(1+\sqrt{1+\rho^2})^2} \tag{4.8a}$$

$$\int \mathrm{d}x \int \mathrm{d}y \, |q_\infty|^2 = 2\ln(1+\rho^2). \tag{4.8b}$$

Here we compare the result of the value $|q_\infty|^2_{\max}$ with that of the simulation given in section 3. The average of the oscillating $|q|^2_{\max}$ in figure 1 is $0.52 \sim 0.54$, and this coincides with the value given in table 1 when the case that a, the amplitude of the Gaussian-type initial condition of q, is 0.4. The results derived from the IST and the direct numerical analysis show good agreement each other. Therefore from these facts we can infer that the oscillation occurring in $|q|^2_{\max}$ in figure 1 subsides in the limit of large t, and a single dromion appears after the radiation goes away.

Table 1. A table of the values of amplitude of the initial condition a, ρ, square amplitude of the initial condition $|a|^2$, the volume of the initial condition V_g, the final square amplitude of dromion $|a_d|^2$, the volume of the final dromion V_d, the amount of ripples V_r and the ratio of V_r against V_g.

a	ρ	$\|a\|^2$	V_g	$\|a_d\|^2$	V_d	V_r	V_r/V_g
0.25	1.016 54	0.0625	1.9635	0.2247	1.4194	0.5441	0.277
0.30	1.340 45	0.0900	2.8274	0.3220	2.0570	0.7704	0.272
0.35	1.742 58	0.1225	3.8485	0.4293	2.7908	1.0577	0.275
0.40	2.247 53	0.1600	5.0264	0.5401	3.6006	1.4258	0.284
0.45	2.886 71	0.2025	6.3617	0.6487	4.4671	1.8946	0.298
0.50	3.700 43	0.2500	7.8538	0.7503	5.3748	2.4790	0.316
0.55	4.740 69	0.3025	9.5033	0.8420	6.3118	3.1915	0.336
0.60	6.074 87	0.3600	11.309	0.9223	7.2701	4.0389	0.357

Since the integral of (3.1) is given by

$$\int \mathrm{d}x \int \mathrm{d}y\, |q|^2 = \frac{\pi a^2}{2\mu} \tag{4.9}$$

the amount of radiation can be calculated by subtracting (4.8*a*) from (4.9). The values are also shown in table 1, together with the ratio of the volume of ripples against the whole volume of the initial wavepacket. From the values of these ratios, we can find the initial wavepacket which is nearest to a dromion. The values listed in the final column of the table 1 show that at the value $a = 0.3$, the initial pulse radiates the least amount of ripple, and this is the pulse closest to the one dromion solution. In addition, they show a tendency that the initial pulse with larger amplitude generates more ripple.

5. Concluding discussions

In this paper, we have investigated the initial-boundary value problem of the DS1 equations both numerically and theoretically. We have performed the numerical analyses in order to clarify the process of emergence of dromions from the initial wavepacket. We have observed that the initial wavepacket grows into a dromion asymptotically with its height oscillating, while ripples run away into the infinity mainly along the mean flows.

If we consider the soliton equations in one dimension, like the KdV and the NLS equations, an initial condition determines the scattering data completely and the scattering data, especially the zeros of the transmission amplitude, determine the number of solitons in the final stage. In the case of the DS1 equations, however, an initial condition determines only ρ, and the number of dromion to appear is determined by the eigenstates of (2.10*b*) under the boundary functions $u(x)$ and $v(y)$. Generally speaking, it is difficult to calculate ρ analytically when the initial condition is given like a Gaussian-type function. Hence in this paper, we have presented the efficient way of calculating the value of ρ numerically in section 4. The results of the simulations are verified by comparing the value of ρ obtained by the direct simulation with the one calculated by the IST. We confirm that these values are approximately the same.

Generally speaking, when we select various values as an initial amplitude of the Gaussian wavepacket, we get different values of ρ. This means that the volume of the final dromion V_d, which is given in (4.8*b*), and that of the initial wavepacket V_g vary correspondingly. This results in the change of the ratio of ripples contained in the initial pulse. The results of

our analyses show that the initial packet with larger amplitude contains more ripples. This ratio can be considered to have a close relation to the parameters λ and μ, defined in (3.1) and (3.2). The study on this relation is a future problem.

Finally, we explain the behaviour of oscillating $|q|^2_{\max}$ shown in figure 1. As we can see from table 1, the maximum amplitude of the final dromion is always larger than that of the initial condition. Thus the height of the initial wavepacket will initially increase in order to attain the final value. Next, it goes past the destined value and begins a damped oscillation around it. This is why an 'oscillating' dromion with ripples appears in the course of time. In the final stage, as predicted by the IST, a single dromion appears at a cross point of mean flows, and the ripples run away into the infinity mainly along the mean flows. This is because the mean flows act as attractive potentials, and this behaviour was also seen in our previous papers [8, 9].

Acknowledgments

The authors are grateful to Professor Junkichi Satsuma for fruitful discussions and helpful comments. They also would like to express their sincere gratitude to Professor Kazumi Watanabe and Dr Yasuhiro Ohta for stimulating discussions and valuable comments.

References

[1] Ablowitz M J and Segur H 1981 *Solitons and the Inverse Scattering Transform* (Philadelphia, PA: SIAM) p 322
[2] Boiti M, Leon J J P, Martina L and Pempinelli F 1988 *Phys. Lett.* **132A** 432
[3] Fokas A S and Santini P M 1989 *Phys. Rev. Lett.* **63** 1329
[4] Davey A and Stewartson K 1974 *Proc. R. Soc.* A **338** 101
[5] Nishinari K Abe K and Satsuma J 1994 *Phys. Plasmas* **1** 2559
[6] Fokas A S and Santini P M 1990 *Physica* **44D** 99
[7] Satsuma J and Yajima N 1974 *Prog. Theor. Phys. Suppl.* **55** 284
[8] Nishinari K and Yajima T 1994 *J. Phys. Soc. Japan* **63** 3538
[9] Nishinari K and Yajima T 1995 *Phys. Rev.* E **51** 4986
[10] Yajima T and Nishinari K 1995 Numerical analyses of the localized structures on an uneven bottom associated with the Davey–Stewartson 1 equations *J. Phys. Soc. Japan* to appear
[11] Santini P M 1990 *Physica* **41D** 26
[12] Sutcliffe P M 1992 *J. Math. Phys.* **33** 2269